



DYNAMICAL SYSTEMS OF DIFFERENT CLASSES AS MODELS OF THE KICKED NONLINEAR OSCILLATOR

A. P. KUZNETSOV and L. V. TURUKINA

*Institute of Radio-Engineering and Electronics of RAS,
Saratov Division, Zelenaya 38, Saratov, Russia*

E. MOSEKILDE

*Department of Physics, Technical University of Denmark,
Build. 309, DK-2800, Kgs. Lyngby, Denmark*

Received May 23, 2000; Revised August 1, 2000

Using the nonlinear dissipative kicked oscillator as an example, the correspondence between the descriptions provided by model dynamical systems of different classes is discussed. A detailed study of the approximate 1D map is undertaken: the period doubling is examined and the possibility of non-Feigenbaum period doubling is shown. Illustrations in the form of bifurcation diagrams and sets of iteration diagrams are given, the scaling properties are demonstrated, and the tricritical points (the terminal points of the Feigenbaum critical curves) in parameter space are found. The congruity with the properties of the corresponding 2D map, the Ikeda map, is studied. A description in terms of tricritical dynamics is found to be adequate only in particular areas of parameter space.

1. Introduction

The first step in studying complex oscillations and chaos in a particular system is the selection of the class of model to be used. Depending on the purpose of the study, this can be a system of differential equations, a 2D map or a 1D (noninvertible) map. The problem of correspondence between different models has been somewhat overshadowed by the idea of Feigenbaum universality and it is commonly thought that realistic systems and complicated mathematical models manifest most of the same regularities as the simplest abstract models like the logistic map. The picture of the transition to chaos via period doublings and the scaling properties at the threshold of chaos will be similar for all models. Renormalization group theory substantiates this fact, and it is also confirmed by numerous investigations of specific examples. However, it should be emphasized that not all phenom-

ena are described by renormalization group theory and lead to period doublings that can be carried over from 1D maps to 2D maps and to continuous-time systems (flows), or vice versa [Kuznetsov *et al.*, 1997a, 1997b; Kuznetsov, 1992]. These behavioral peculiarities reveal themselves under two-parameter analysis. For example, for 1D maps, the curve which corresponds to transition to chaos can terminate at tricritical points [Chang *et al.*, 1981]. For 2D maps (and for flows), tricritical points of this type are not observed [Kuznetsov *et al.*, 1997a, 1997b; Kuznetsov, 1992]. The corresponding structure of parameter space appears to be realized only approximately, at some level of refinement. Thus, two-parameter analysis of the dynamics of a particular system requires careful control of the ability of the dynamical model to describe the phenomena of interest and a discussion of the correspondence between the descriptions at different levels of precision.

A very convenient subject for research on this problem is provided by kicked systems, because they allow advanced analytical investigations. The bouncing ball [Bergé *et al.*, 1984; Moon, 1987; Guckenheimer & Holmes, 1983], the kicked rotator [Schuster, 1984], the damped mathematical pendulum that rotates between electromagnetic poles [Heagy, 1992], etc., all belong to this class of systems. The present work is devoted to investigating the nonautonomous dissipative kicked oscillator. Using the method of slow amplitudes we obtain a model 2D map. This map coincides with one of the well-known models of nonlinear dynamics, the Ikeda map. The one-dimensional approximation yields the “cosine map”. Our purpose is to perform a comparison of the descriptions in terms of these models.

In the present work the nonlinear oscillator is an instrument rather than an object of research. Nevertheless, let us say a few words about the modeling of a kicked oscillator by 2D maps. Parlitz suggested that the description of the complex dynamics demonstrated by a periodically driven oscillator is an advanced model in the form of a 2D “twist-and-kick map” [Parlitz, 1993; Parlitz *et al.*, 1991]. But the main emphasis of their work was devoted to other problems. They limited their consideration to establishing the fact, that both oscillator and its model exhibit the “crossroad area” and “spring area” structures [Carcasses *et al.*, 1991] in parameter space. We think, that this is not sufficient when comparing dynamical systems of different classes. More detailed two-parameter investigations are necessary.

2. From Flow to Two-Dimensional Map

Let us consider a periodically kicked dissipative oscillator with cubic nonlinearity. The behavior of such a system can be described by the following differential equation:

$$\ddot{x} + \gamma\dot{x} + \omega_0^2 x + \beta x^3 = \sum_n C\delta(t - nT) \quad (1)$$

where x is the coordinate of the oscillator, γ the parameter of dissipation, and ω_0 the oscillator frequency. T is the interval between the kicks, and C is their amplitude.

At first, we shall obtain a 2D map for the system at issue. The right-hand part of Eq. (1) van-

ishes between the kicks. Hence, we can find an approximate analytical solution by using the method of slow amplitudes. Let us express x in the following form:

$$x = \frac{a}{2}e^{i\omega_0 t} + \frac{a^*}{2}e^{-i\omega_0 t}, \quad (2)$$

where $a = a(t)$ is the slowly varying amplitude of the oscillator. The asterisk denotes complex conjugate. Substituting this expression into Eq. (1) and accounting for the additional condition

$$\dot{a}e^{i\omega_0 t} + \dot{a}^*e^{-i\omega_0 t} = 0, \quad (3)$$

after averaging over time we obtain the following truncated equation:

$$\dot{a} = -\frac{\gamma}{2}a + \frac{3i\beta}{8\omega_0}|a|^2 a. \quad (4)$$

Let us introduce the real amplitude R and phase φ by using the substitution $a = Re^{i\varphi}$. By separating real and imaginary parts in Eq. (4) we arrive at the following expressions:

$$\dot{R} = -\frac{\gamma}{2}R, \quad (5)$$

$$\dot{\varphi} = \frac{3\beta}{8\omega_0}R^2. \quad (6)$$

Solving these equations we find the amplitude and phase between the n -th and $(n+1)$ -th kicks as functions of time as

$$R(t) = R_n e^{-\gamma t/2}, \quad (7)$$

$$\varphi(t) = \frac{3\beta}{8\omega_0}R_n^2 \frac{1 - e^{-\gamma t}}{\gamma} + \varphi_n. \quad (8)$$

Here R_n and φ_n are the initial amplitude and phase, immediately after the n -th kick.

From Eqs. (2) and (3) we obtain the following relations:

$$x(t) = R(t) \cos(\omega_0 t + \varphi(t)), \quad (9)$$

$$v(t) = -\omega_0 R(t) \sin(\omega_0 t + \varphi(t)). \quad (10)$$

Substituting (7) and (8) into (9) and (10) we find the oscillator coordinate and velocity as functions of time. The time interval between the n -th and $(n+1)$ -th kicks is T . Therefore the coordinate and velocity before the $(n+1)$ -th kick are given by $x(T)$ and $v(T)$, respectively. Immediately after the $(n+1)$ -th kick the coordinate is not changed, while the velocity is changed by the addend C , because

the force pulse is the delta function. Therefore, for the coordinate and velocity immediately after the $(n + 1)$ -th kick we obtain the following expressions:

$$x_{n+1} = R_n e^{-\gamma T/2} \cos \left(\omega_0 T + \frac{3}{8} \frac{\beta}{\omega_0} |R_n|^2 \frac{1 - e^{-\gamma T}}{\gamma} + \varphi_n \right), \quad (11)$$

$$v_{n+1} = -\omega_0 R_n e^{-\gamma T/2} \sin \left(\omega_0 T + \frac{3}{8} \frac{\beta}{\omega_0} |R_n|^2 \frac{1 - e^{-\gamma T}}{\gamma} + \varphi_n \right) + C. \quad (12)$$

It is convenient to rewrite these relations in complex form. We introduce the complex variable as:

$$z = \left(ix + \frac{v}{\omega_0} \right) \sqrt{\frac{3}{8} \frac{\beta}{\omega_0} \frac{1 - e^{-\gamma T}}{\gamma}}. \quad (13)$$

Then, taking (9) and (10) into account, from (11) and (12) we obtain the map for the variable z :

$$z_{n+1} = A + B z_n \exp(i(|z_n|^2 + \psi)), \quad (14)$$

where the new parameters A , B , and ψ are determined by the initial system parameters as follows:

$$A = \frac{C}{\omega_0} \sqrt{\frac{3}{8} \frac{\beta}{\omega_0} \frac{1 - e^{-\gamma T}}{\gamma}}, \quad B = e^{-\gamma T/2}, \quad \psi = \omega_0 T. \quad (15)$$

Note, that the same map was suggested by Ikeda for an optical ring cavity with a nonlinear medium [Ikeda *et al.*, 1980]. Thus, the map (14) allows various physical interpretations. This is not so surprising, because we used very general assumptions to deduce it.

The Ikeda map (14) is one of the standard models of nonlinear dynamics. For example, in a recent survey [Mosekilde, 1996] one can find detailed bifurcation analysis for it. As a complement to these results, we present here the topography of dynamical regimes for the Ikeda map for the parameter value $\psi = 0$ [Fig. 1(a)]. In this and the analogous charts to follow, the regions of periodic behavior with different periods are shown with different colors, for instance 1 is green, 2 is yellow, 3 is magenta, 4 is blue, while the gray color represents chaos. Note, that in some regions multistability occurs. The charts of dynamical regimes have to be regarded not as one “sheet”, but as a set of “sheets”, which overlap in the region where the system has more than one attractor. At the boundaries of the “sheets” the system exhibits a jump from one “sheet” to another. Straightforward plotting of the diagram does not reveal all the “sheets”, but in any case the charts obtained are useful for understanding the dynamics. In the parameter plane one can find a set of cusp points with lines of tangent bifurcations emanating from them, as well as various regions of cycles of doubled period. The region of chaos

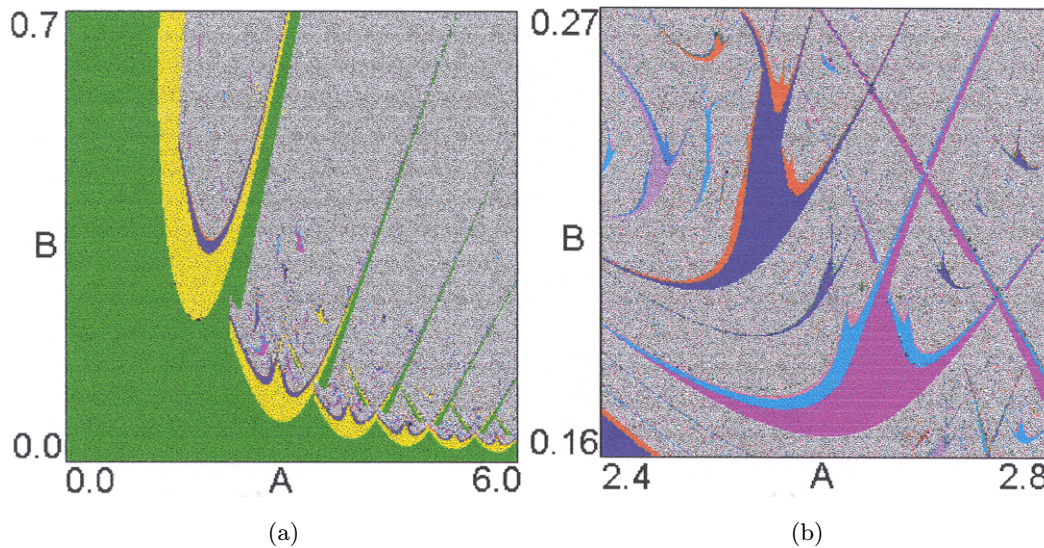


Fig. 1. Topography of the dynamical regimes in parameter space for the Ikeda map. (a) For the case $\omega = 0$ (b) fragment of the first figure.

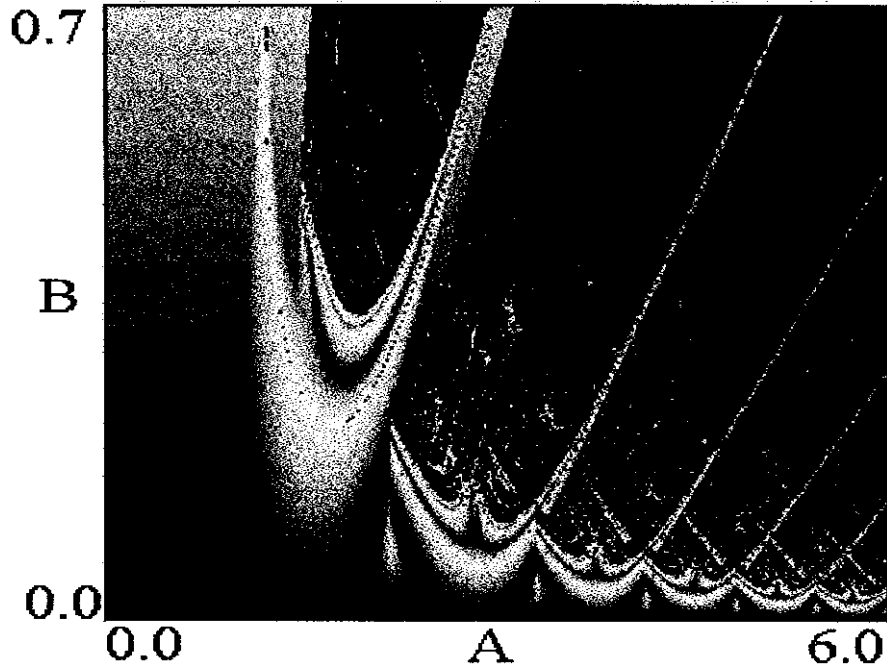


Fig. 2. Topography of the largest Lyapunov exponent for the Ikeda map.

contains structures typical for two-parameter systems which are called “crossroad areas” [Carcasses *et al.*, 1991]. This is a typical composition of lines of tangent bifurcation and of period doubling. A number of such structures are observed in Fig. 1(b). They are based on the low-periodic cycles. Note, that charts of the dynamical regimes for other

values of the phase parameter do not differ qualitatively from the above.

Together with charts of the dynamical regimes, we plot charts of the largest Lyapunov exponent for the Ikeda map (Fig. 2). In this diagram the change of the largest Lyapunov exponent from minus infinity to zero corresponds to the change of

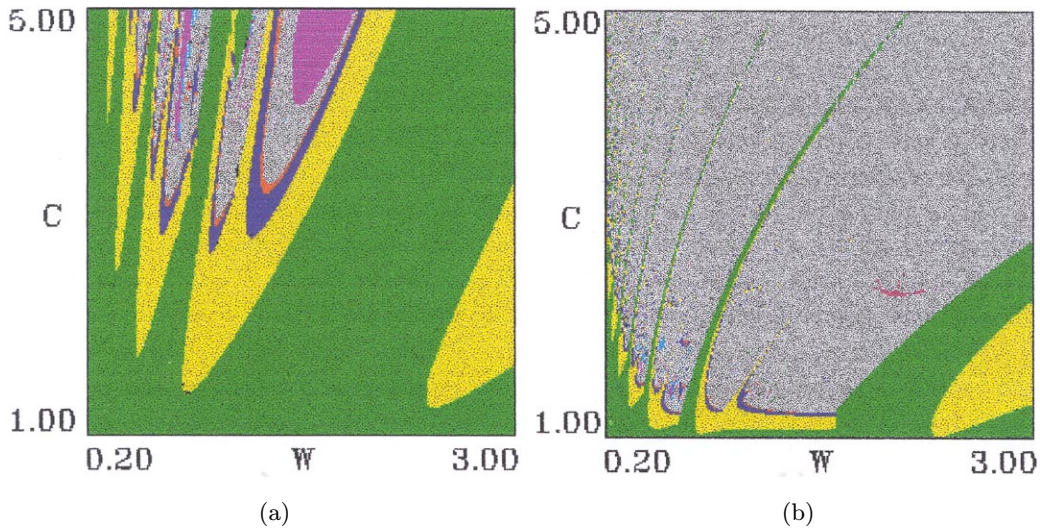


Fig. 3. Comparison of the topographies of the dynamical regimes for the differential equation and the 2D map in the parameter space (C, W) : (a) Topography for the oscillator for $\beta = 1$ and $\gamma = 0.2$, (b) topography for the Ikeda map for the same parameter values, (c) topography for the oscillator for $\beta = 1$ and $\gamma = 0.05$, and (d) topography for the Ikeda map for the same parameter values.

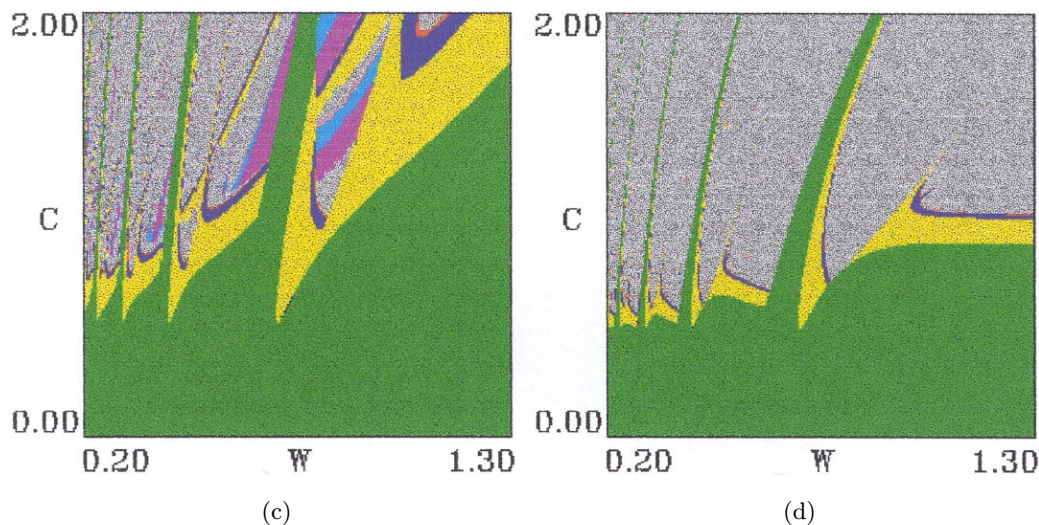


Fig. 3. (Continued)

color from dark gray to white, while the black color corresponds to positive values.

Now let us discuss the question of correspondence between the descriptions of the original system by the differential equation (1) and by the 2D map (14). With this aim we display charts of the dynamical regimes for the oscillator and for the 2D map in the parameter space of the oscillator. These charts are shown in Fig. 3. Here $W = 2\pi/T$ is the kick frequency and, as before, C is the amplitude. The charts of dynamical regimes for the original differential system (1) are shown in the left column. These charts are obtained by the method of Poincaré mapping. The charts of dynamical regimes for the 2D map (14) are shown to the right. Note, that the parameters of the 2D map are converted by using relations (15) and that the frequency of the oscillator is $\omega_0 = 1$.

In the diagrams one can find a set of cusp points with lines of tangent bifurcations going out from them. These points correspond to resonances in the nonautonomous oscillator at its own frequency and at its subharmonics. There is a complex picture of different dynamical regimes in the region of each resonance.

One can see that the correspondence between the charts of dynamical regimes for the value of the dissipation parameter $\gamma = 0.2$ is unsatisfactory. This means, that such a value of dissipation is too big for the method of slow amplitudes to be valid. For $\gamma = 0.05$, however, one can see a more acceptable correspondence, especially in the region of

resonance at far subharmonics, i.e. in the region of small frequencies. With a smaller frequency of the kicks, the oscillator performs more oscillations between the kicks, and the method of slow amplitudes is more effective.

3. One-Dimensional Map

It is necessary to have a strong compression of the cloud of points in phase space (i.e. the system must be strongly dissipative) in order for the 1D map to approximate the 2D map adequately. At first sight this contradicts the condition of applicability of the method of slow amplitudes that we have used in the previous section. In accordance with Eq. (15), however, parameter B is decreased when we move to the region of the resonance at subharmonics (i.e. to the region where the method of slow amplitudes is working). In addition, as we shall show in Sec. 4, there are other reasons for the 1D map to work well in this case.

Let us plot the attractor for the 2D map at different points of parameter space (Fig. 4). Inspection of the figure shows that the attractor has a two-dimensional structure when parameter A is small and parameter B is sufficiently large, while it attains a one-dimensional structure as parameter A is increased and parameter B decreased. The same general tendency is observed for other values of the parameters A and B . Thus, the 2D map can be reduced to a 1D map when the condition $B \ll A$ is satisfied.

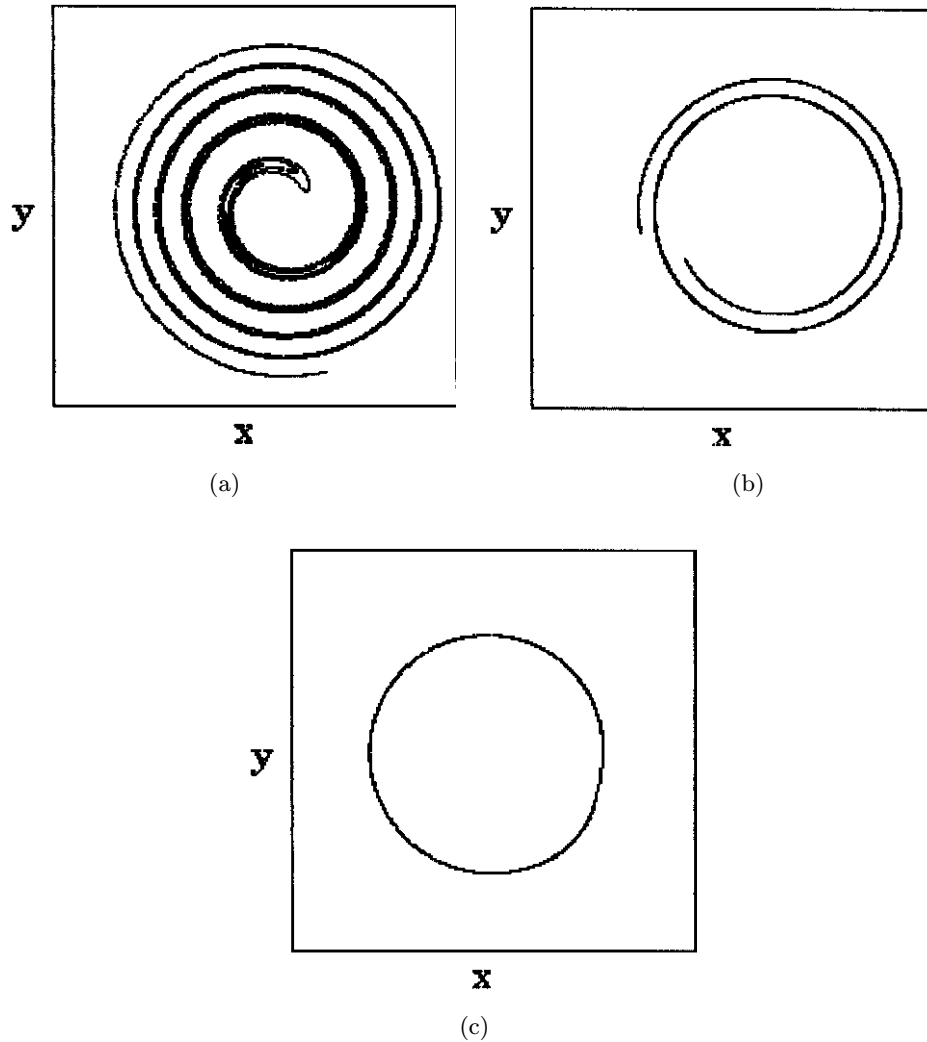


Fig. 4. Attractors for the Ikeda map in phase space for the cases: (a) $A = 3.240$, $B = 0.445$, (b) $A = 4.70$, $B = 0.126$, and (c) $A = 5.240$, $B = 0.056$.

Let us construct the corresponding 1D map. Following [Carr & Eilbech, 1984] let us suppose that B is small. Then we can present the variable z in the form $z = A + \tilde{z}$ where \tilde{z} is small. From Eq. (14) we have for the variable \tilde{z} :

$$\tilde{z}_{n+1} = AB \exp(i(A^2 + A(\tilde{z}_n + \tilde{z}_n^*) + \psi)). \quad (16)$$

Let $x = A^2 + A(\tilde{z} + \tilde{z}^*) + \psi$. Then for the variable x we obtain the following 1D map:

$$x_{n+1} = \lambda \cos(x_n) + \varphi, \quad (17)$$

where the new parameters λ and φ are determined in terms of the 2D map parameters as follows:

$$\lambda = 2A^2B \quad \varphi = A^2 + \psi. \quad (18)$$

This passage to a 1D map implies a reduction of the number of relevant parameters from 3 to 2.

The 1D map (17) is represented by a very simple expression. It should be noted, however, that this map is an interesting object by itself. For example, it can be used to describe an acousto-optical system with delay [Vallee *et al.*, 1984].

Let us discuss now the complex dynamics of the 1D map. The topography of dynamical regimes for the 1D map is presented in Fig. 5(a), and the topography of the largest Lyapunov exponent is presented in Fig. 5(d). In these charts one can see objects of the same type as for the Ikeda map. There are lines of tangent bifurcations, regions of the period doubled cycles, fragments containing the “crossroad area”, etc.

The 1D map (17) demonstrates the well-known Feigenbaum scenario [Bergé *et al.*, 1988; Moon, 1987; Guckenheimer & Holmes, 1983]. In Fig. 6 the bifurcation tree is presented, values of x are plotted

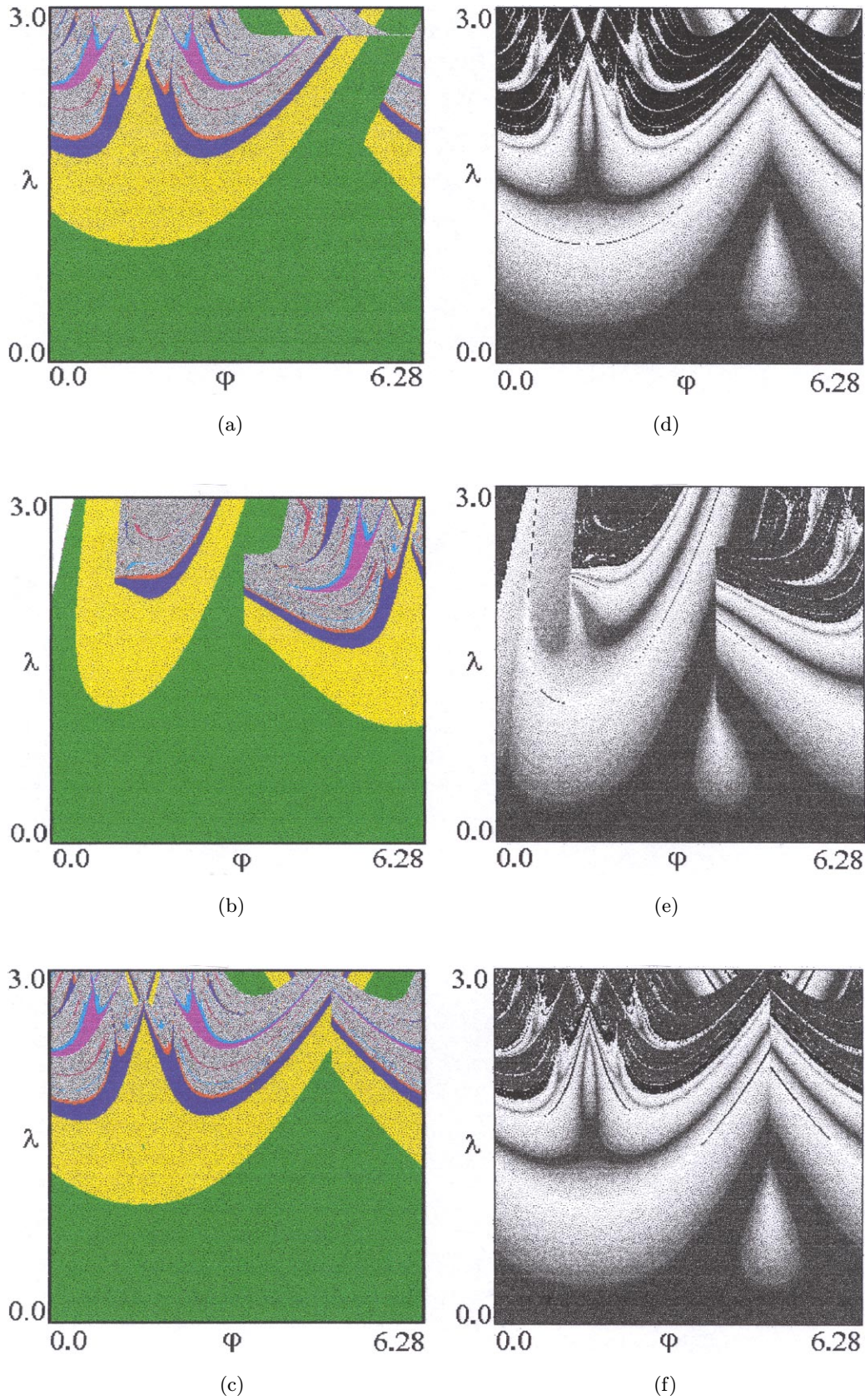
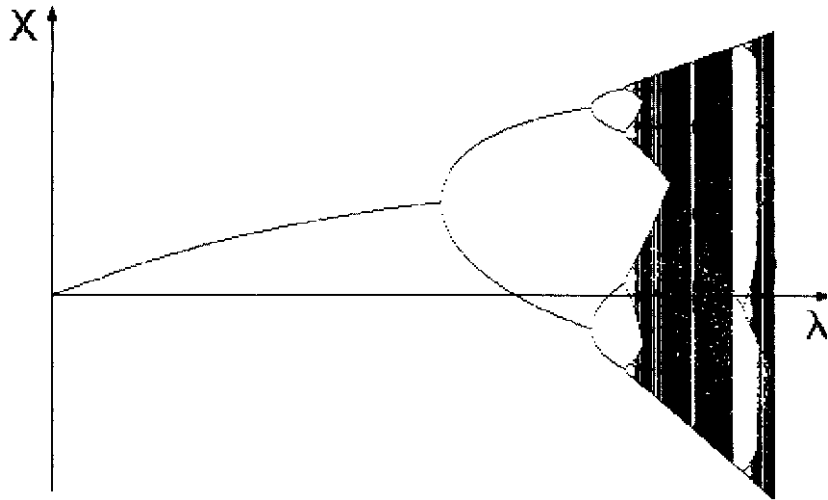
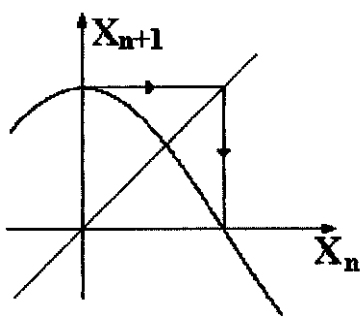


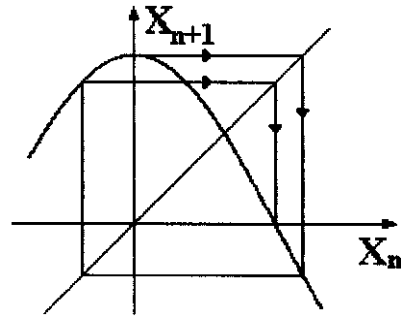
Fig. 5. Comparison of the topography of the dynamical regimes and the topography of the largest Lyapunov exponent for 2D and 1D maps in the parameter space (λ, φ) : (a, d) Topography for 1D map, (b, e) topography for 2D map for small values of parameter A , and (c, f) for sufficiently large values of A .



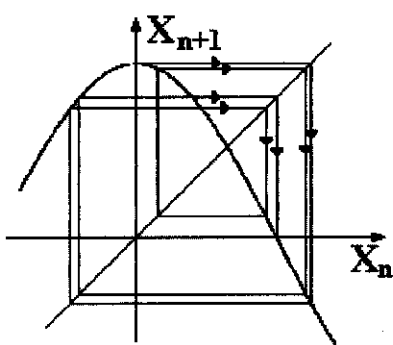
(a)



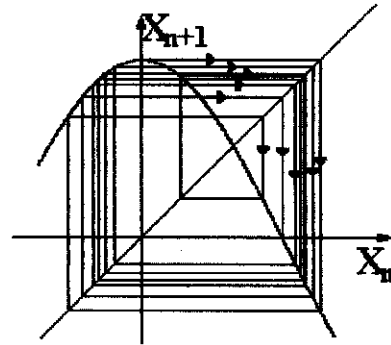
(b)



(c)



(d)



(e)

Fig. 6. (a) Bifurcation diagram for the cosine map (17) in the case $\varphi = 0$. (b-e) Iteration diagrams for the superstable cycles of period 2-16; parameter values $\lambda = 1.57079633$, $\lambda = 1.88740798$, $\lambda = 1.95565631$ and $\lambda = 1.99763129$.

versus λ along the line $\varphi = 0$, and the set of iteration diagrams is given for the superstable cycles in this case. The superstable cycles contain the point of the extremum. The corresponding sequence of λ converges to the limit value according to the geometrical law with the universal Feigenbaum factor $\delta = 4.669\dots$

The Feigenbaum scaling properties for the bifurcation tree and for the largest Lyapunov exponent are illustrated in Fig. 7.

However, the 1D map (17) demonstrates non-Feigenbaum period doubling cascades as well. One of them is observed along the line $\lambda = \pi - \varphi$, which corresponds to mapping the maximum onto the

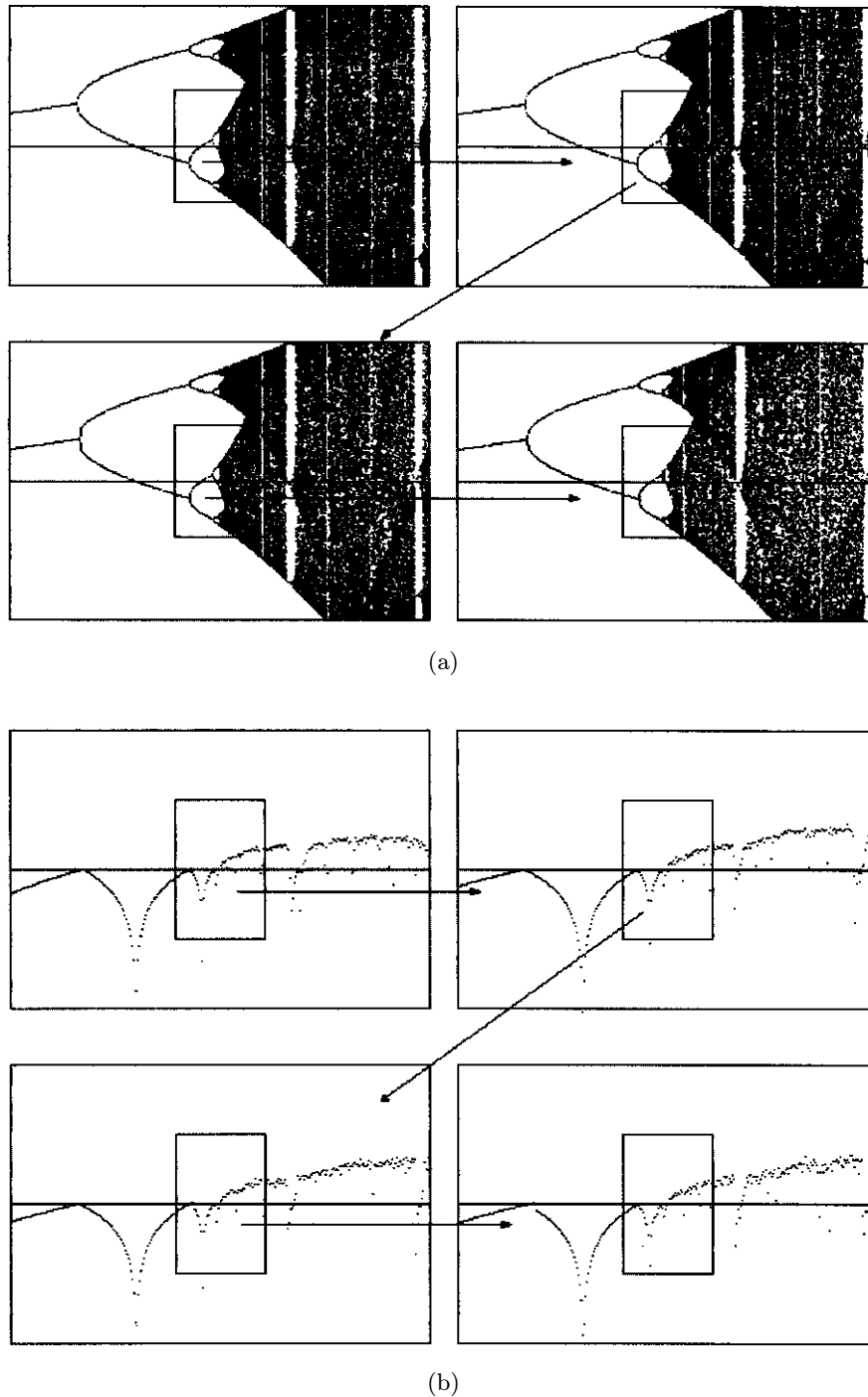
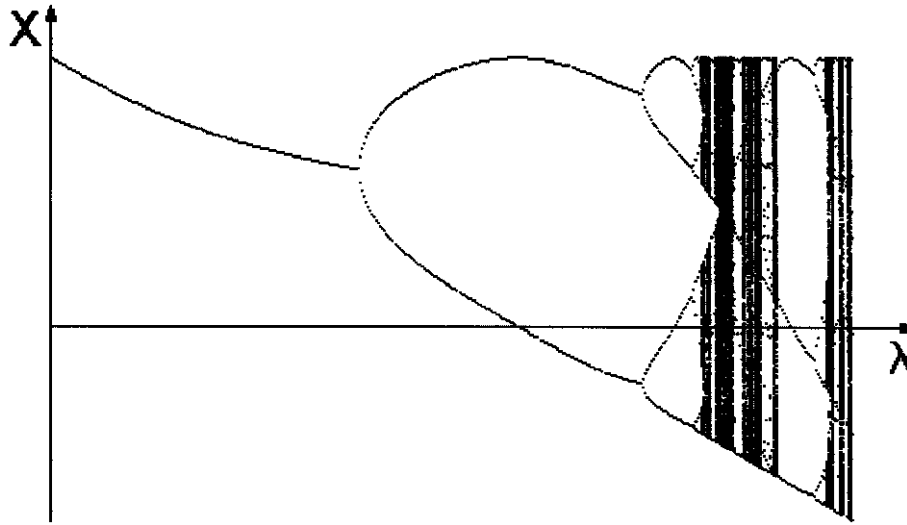


Fig. 7. Scaling on (a) the bifurcation diagram and on (b) the diagram of the largest Lyapunov exponent for $\varphi = 0$.

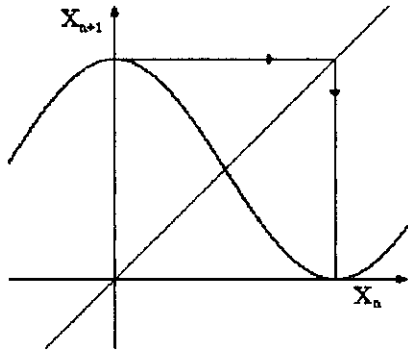
minimum. Figure 8 illustrates the bifurcation diagram and the set of iteration diagrams for the superstable cycles in this case. Note that the bifurcation diagram differs from the bifurcation diagram in the previous case. For example, it has wider periodic windows. Now the superstable cycles involve two extrema, and the corresponding values of parameter λ accumulate at the point $\lambda_T = 2.18603861533$ with

another universal factor $\delta \simeq 7.28469$. These points are called tricritical points by Chang *et al.* [1981]. They are terminal points of Feigenbaum's critical curves in parameter space [Kuznetsov *et al.*, 1997a, 1997b].

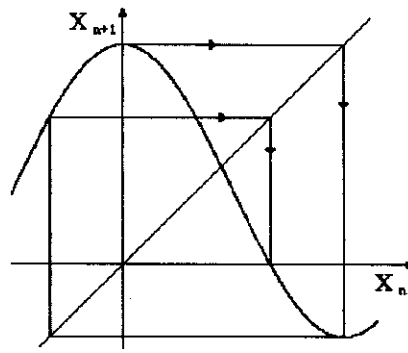
The 1D map also demonstrates non-Feigenbaum period doubling along the line $\lambda = \varphi$, which corresponds to mapping the minimum onto



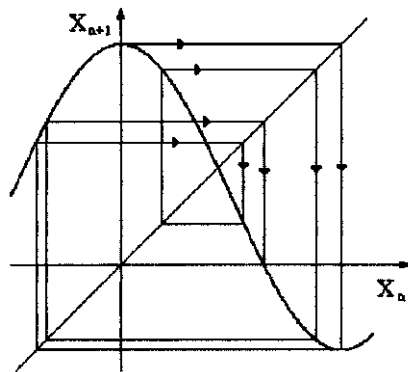
(a)



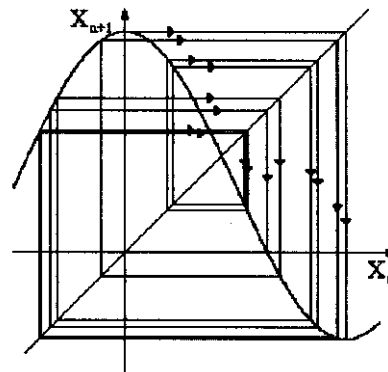
(b)



(c)



(d)



(e)

Fig. 8. (a) Bifurcation diagram for the cosine map (17) in the case $\lambda = \pi - \varphi$. (b–e) Iteration diagrams for the superstable cycles of period 2–16; parameter values $\lambda = 1.57000100$, $\lambda = 2.09330461$, $\lambda = 2.17229248$ and $\lambda = 2.18319192$.

the maximum. Figure 9 illustrates “portraits” of attractors at the tricritical points for both cases. Figure 10 shows the scaling on the diagrams of the largest Lyapunov exponent in the case $\lambda = \pi - \varphi$.

4. From 1D Map to 2D Map

Let us discuss the correspondence between the descriptions of dynamics in terms of the 1D map (17)

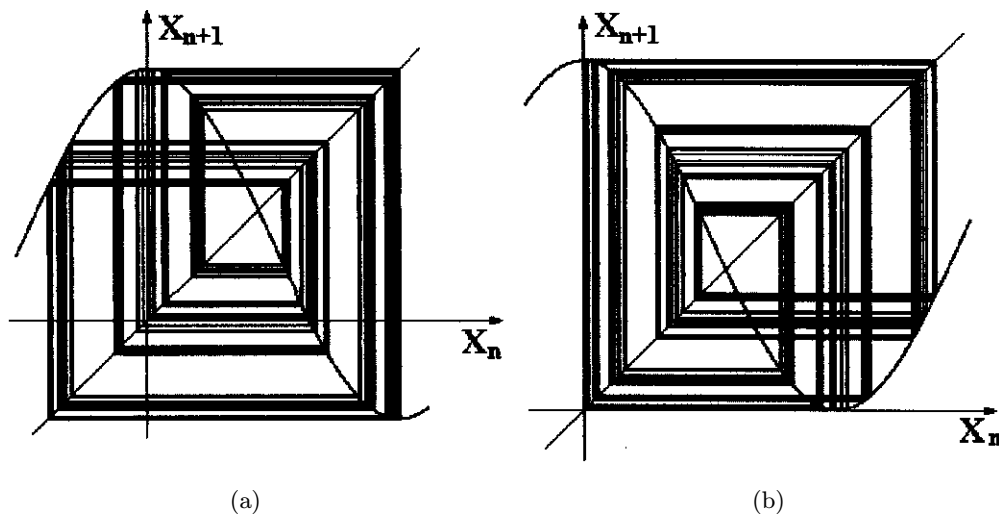


Fig. 9. “Portraits” of attractors at the tricritical point $\lambda = 2.18603861533$ for the map (17) in the cases (a) $\lambda = \pi - \varphi$ and (b) $\lambda = \varphi$.

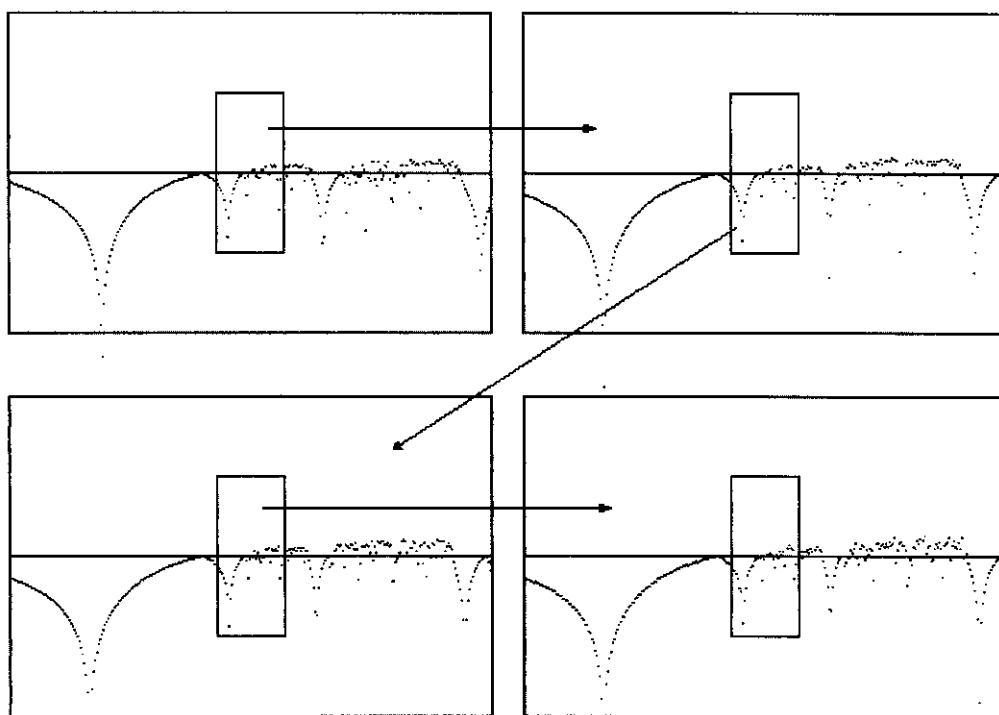


Fig. 10. Scaling on the diagram of the largest Lyapunov exponent for $\lambda = \pi - \varphi$.

and the 2D map (14). First, we compare the charts of dynamical regimes in the parameter space of the 1D map (λ, φ) for both cases. Note, that the cosine is a periodic function, therefore the parameter space for the 1D map has a periodic structure. (The part presented in Fig. 5(a) corresponds to the phase φ changing from 0 to 2π .) This allows us to choose elementary “cells” in the diagram for the

Ikeda map [Fig. 11(a)]. They are regions bounded by the following lines: $B = \lambda/2A^2$, where $\lambda = 3$ corresponds to the upper boundary of the chart of the 1D map. $A = \sqrt{2\pi(n-1)}$ and $A = \sqrt{2\pi n}$, respectively, where n is the number of “cells” [see the Fig. 11(a)].

Let us now consider in detail the region 1, which corresponds to small values of A , and the region 3,

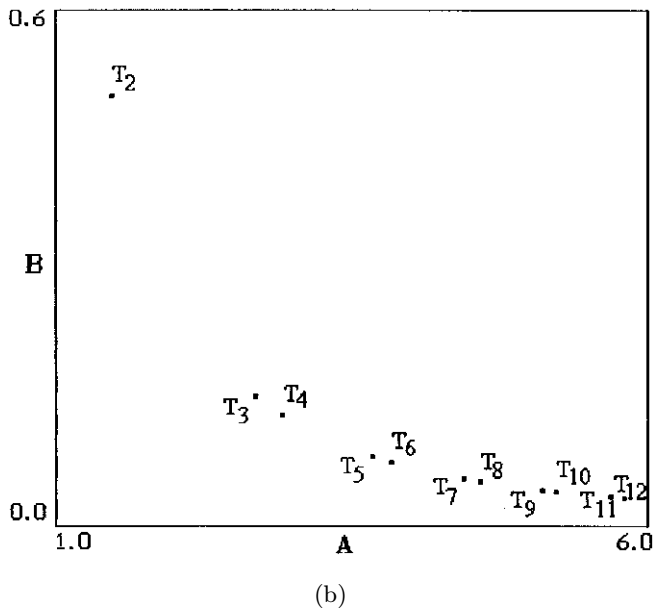
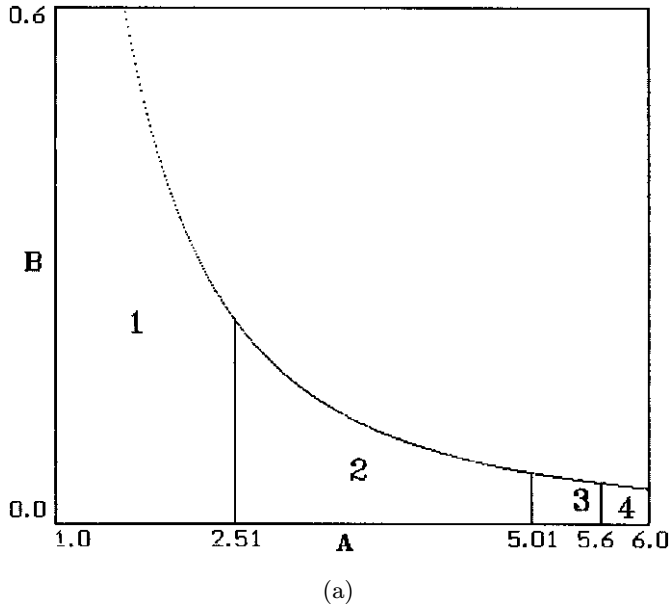


Fig. 11. Parameter space for the Ikeda map: (a) Each region corresponds to a fragment of the parameter space for the 1D map Fig. 3(a). (b) Set of tricritical points in the parameter space (A, B) as predicted on the basis of the 1D model.

which corresponds to larger A . We can apply the transformation rule (18), obtain the charts for the 2D map in the new coordinate system (λ, φ) , and then compare them with the charts for the 1D map (17) [see Figs. 5(a)–5(c)]. From this comparison it follows, that the picture obtained for the first region [Fig. 5(b)] looks rather distinct from the topography of the 1D approximate map [Fig. 5(a)], while the picture obtained for the third region [Fig. 5(c)] is similar to that for the 1D map. One can make a

similar comparison for the topography of the largest Lyapunov exponent. Such pictures are presented in Figs. 5(d)–5(f).

From our derivation of the 1D map it follows that the adequacy of the 1D map is determined by the degree to which the condition $B \ll A$ is fulfilled. When we consider “cells” with higher and higher numbers, parameter B is reduced and parameter A is increased. So it is clear, that the one-dimensional approximation becomes more precise. Under these conditions, corresponding to Figs. 5(b) and 5(e), we have B about 0.3 and A about 1.5, while in the case of Figs. 5(c) and 5(f), B is about 0.05 and A is about 5.

As already noted, tricritical points (the terminal points for the curves of Feigenbaum’s transition to chaos) are very typical points for 1D maps. We have found two such points for the 1D map (17) which correspond to mapping the maximum into the minimum and vice versa. We can determine the corresponding points in the parameter space (A, B) for the 2D map (14) using the relations (18). In Fig. 11(b) these points are plotted in the parameter plane for the 2D map. Note, that instead of two points we have a set of points, because the cosine is a periodic function. The region around each pair of these points is shown in Fig. 5(a) for the 1D map. By comparison of Figs. 11(b), 5(a) and 1, we can see that this configuration, which demonstrates a typical structure of parameter space, is present for the 2D map.

However, on the basis of the renormalization group approach one can prove, that tricritical points in the parameter space do not survive after the second dimension is involved. They are actualized only in some restricted sense, up to a definite level of refinement [Kuznetsov *et al.*, 1997a, 1997b; Kuznetsov, 1992]. Thus, the corresponding universal configuration of the parameter space in the vicinity of the tricritical point is destroyed when we observe the chart for the 2D map with sufficient resolution. The better the 1D approximation is, the deeper can we observe the tricritical behavior. It follows from comparison of Figs. 5(a) and 5(b), that for the first “cell” this configuration is already destroyed.

5. Conclusion

In the present work three relevant classes of dynamical systems were examined. We derived 2D and 1D

maps for the nonlinear dissipative kicked oscillator with cubic nonlinearity, and the topography charts of dynamical regimes were plotted for all models. The topography charts for the largest Lyapunov exponents were presented for 1D and 2D maps, and we discussed the correspondence between these charts.

What we have established, primarily, is that for systems with complex dynamics, we must discuss not only physical reasons to use one or another approximation, but also the presence of phenomena of complex dynamics must be taken into account. Especially this concerns the global bifurcation picture, the points and lines at which the bifurcations accumulate. The situation becomes complicated, when we consider the regions with the most complex organization. Universality of nonlinear dynamical phenomena at the onset of chaos is not so simple as in the one-parameter case.

In the case at issue, when we turn from the description in terms of differential equations to 2D maps, the efficiency of the approximated method is lower than when we go from a 2D map to a 1D map. The fine-scale structure of long-periodical regions in the parameter space near the resonances (the cusp points) is badly reproduced in the frequency–amplitude parameter plane of the oscillator, while for the 2D map the fine-scale structure in the vicinity of the cusp points is well described by the 1D map.

Our investigations confirm a conclusion from the renormalization group theory that the correlation between 1D and 2D maps is trivial only in the case of one-parameter analysis. The Feigenbaum universality is the same in both cases. On the other hand, for 1D map the points are typical which are the accumulation points for the “crossroad areas” based on the increasing period cycles. These points are the terminal points of the Feigenbaum critical curves in parameter space. Their vicinities are universally structured. For 2D maps the corresponding picture arises only in the form of some intermediate asymptotics. However, it can have a very high similarity. Therefore even a glance at the topography of the dynamical regimes of a 2D map can reveal the corresponding regions in the parameter space and allow us to judge the sufficiency of a one-dimensional approximation. Certainly, this is important qualitative information in the investigation of new systems.

Acknowledgments

The authors wish to thank S. P. Kuznetsov for help and discussions. The work was supported in part by grant of “Integration” Federal Program 696.3 and by grant of Ministry of Education of RF 97-0-8.3-88.

References

- Bergé, P., Pomeau, I. & Vidal, Ch. [1984] *Order within Chaos: Towards a Deterministic Approach to Turbulence* (Wiley and Sons, NY).
- Carcasses, J., Mira, C., Bosch, M., Simo, C. & Tatjer, J. C. [1991] “Crossroad area–spring area transition (I) parameter plane representation,” *Int. J. Bifurcation and Chaos* **1**, 183–196.
- Carr, Y. & Eilbech, Y. C. [1984] “One-dimensional approximations for a quadratic Ikeda map,” *Phys. Lett.* **A104**, 59–62.
- Chang, S. J., Wortis, M. & Wright, J. A. [1981] “Iterative properties of a one-dimensional quartic map. Critical lines and tricritical behaviour,” *Phys. Rev.* **A24**, 2669–2684.
- Guckenheimer, J. & Holmes, Ph. [1983] *Nonlinear Oscillations, Dynamical Systems and Bifurcations of Vector Fields* (Springer-Verlag, NY).
- Heagy, J. F. [1992] “A physical interpretation of the Hénon map,” *Physica* **D57**, 436–446.
- Ikeda, K., Daido, H. & Akimoto, O. [1980] “Optical turbulence: Chaotic behavior of transmitted light from a ring cavity,” *Phys. Rev. Lett.* **45**, 709–712.
- Kuznetsov, A. P., Kuznetsov, S. P. & Sataev, I. R. [1997a] “A variety of period-doubling universality classes in multi-parameter analysis of transition to chaos,” *Physica* **D109**, 91–112.
- Kuznetsov, A. P., Kuznetsov, S. P. & Sataev, I. R. [1997b] “Codimension and typicality in the context of description of transition to chaos via period-doubling in dissipative dynamical system,” *Regular & Chaotic Dyn.* **2**, 90–105.
- Kuznetsov, S. P. [1992] “Tricriticality in two-dimensional maps,” *Phys. Lett.* **A169**, 438–444.
- Moon, F. [1987] *Chaotic Vibrations* (Wiley and Sons).
- Mosekilde, E. [1996] *Topics in Nonlinear Dynamics* (World Scientific, Singapore).
- Parlitz, U., Scheffczyk, C., Kurz, T. & Lauterborn, W. [1991] “On modeling driven oscillators by maps,” *Int. J. Bifurcation and Chaos* **1**, 261–264.
- Parlitz, U. [1993] “Common dynamical features of periodically driven strictly dissipative oscillators,” *Int. J. Bifurcation and Chaos* **3**, 703–715.
- Schuster, H. G. [1984] *Deterministic Chaos* (VCH Verlagsgesellschaft, Weinheim).
- Vallee, R., Delisle, C. & Chrostowski, J. [1984] “Noise versus chaos in an acousto-optic bistability,” *Phys. Rev.* **A30**, 336–342.